J. Appl. Comput. Mech., 8(4) (2022) 1370-1386
DOI: 10.22055/jacm.2022.40148.3529

ISSN: 2383-4536
jacm.scu.ac.ir

Shahid Chamran University of Ahvaz

Journal of Applied and Computational Mechanics

Research Paper

On the Thermo-elastic Response of FG-CNTRC Cross-ply Laminated Plates under Temperature Loading using a New HSDT

Attia Bachiri[1,2], Ahmed Amine Daikh[3,4], Abdelouahed Tounsi[2,5,6]

[1] Water Resources, Soil and Environment Laboratory, Civil Engineering Department, Faculty of Architecture and Civil Engineering, University of AT, Laghouat, Ghardaia Road BP 37G, Algeria, Email: attia.bachiri@lagh-univ.dz

[2] Material and Hydrology Laboratory, University of Sidi Bel Abbes, Faculty of Technology, Algeria

[3] Department of Technology, University Centre of Naama, Naama 45000, Algeria, Email: daikh.ahmed.amine@gmail.com

[4] Structural Engineering and Mechanics of Materials Laboratory, Department of Civil Engineering, Mascara, Algeria

[5] Department of Civil and Environmental Engineering, King Fahd University of Petroleum & Minerals, 31261 Dhahran, Eastern Province, Saudi Arabia

[6] YFL (Yonsei Frontier Lab), Yonsei University, Seoul, Korea, Email: tou_abdel@yahoo.com

Received February 26 2022; Revised April 21 2022; Accepted for publication April 27 2022.
Corresponding author: A. Bachiri (attia.bachiri@lagh-univ.dz)

Abstract. In this paper, we present a mathematical model based on the new higher shear deformation plate theory to investigate the thermo-elastic response of carbon nanotube reinforced composites (CNTRC) cross-ply laminated plates under temperature loading. Functionally graded distributions (FG) and uniform distribution (UD) of carbon nanotube reinforcement material are examined. A higher-order deformation plate that contains only four unknowns is utilized together with the principle of virtual displacement to derive the governing equations of CNTRC cross-ply laminated plates with simply supported edge conditions. Subsequently, Navier's solution is proposed for simply supported cross-ply CNTR composite laminated plates subject to linear, nonlinear and combined variations in temperature through plate thickness. The analytical model was validated by comparing the obtained primary outcomes with those available in the literature. The numerical results of present simple analytical model are presented to show the influence of the CNT volume fraction, laminated composite structure, side to thickness and aspect ratio on the thermal stresses and deflection of the CNTRC cross-ply laminated plates.

Keywords: Bending; Carbon nanotube reinforced composites; laminated plates; higher-order deformation plate theory; temperature loading.

1. Introduction

Composite materials are obtained from a combination of two or more materials on a microscopic scale. They are widely used in automobile, marine, aerospace, civil engineering and other industries because of their better properties like stiffness, strength, low weight, corrosion resistance, thermal properties, fatigue life and wear resistance [1-3]. The main constituents of the composite materials are fiber and matrix. The fibers are used because of their high specific mechanical properties compared to those of traditional bulk materials. Recently, carbon nanotubes namely CNTs were considered an excellent alternative to classical fiber reinforced composites, due to their perfect bonding with the polymeric isotropic matrix [4-8]. CNTs can be categorized as single walled carbon nanotubes (SWCNT) and multi-walled carbon nanotubes (MWCNT). SWNTs are nanometer diameter cylinders made up of a single rolled up graphene sheet to form a tube and MWCN consists of multiple rolled up graphene sheets to form a tube. They have low density and high stiffness and strength aspect ratios (strengthening 20 times that of high strength steel alloys, half denser than aluminum) [9-11]. It was discovered that dispersing just the 1 wt% of multi walled carbon nanotubes (MWCNTs) homogeneously distributed within the polystyrene matrix, resulted in (36-42%) increase in Young's modulus and in the 25% increase of the breaking stress [12]. The CNTs can be uniformly distributed through the layer thickness or functionally graded. The nanoscale effect of the CNT is taken into account by considering the efficiency parameters of the CNT, these parameters may be calculated by comparing the elastic coefficients computed by the molecular dynamics simulation with the coefficients calculated by the rule of mixture [13]. Recently, many scientists are using molecular dynamics (MDs) as a new procedure to model for nanostructures and microstructures materials; the latter is a powerful alternative to reduce experimental costs in laboratory evaluation, as it has been used in many medical and technical engineering disciplines [14].

Thanks to its important structural performance, reinforced single-layer carbon nanotubes composite plates have been extensively studied by authors in recent decades. For the first time, Popov et al. [15] evaluated the elastic properties of triangular, close-packed crystal lattices of SWCNTs using analytical expressions based on a force-constant lattice dynamical model; a

Published online: May 10 2022

modified power law was used to describe the distribution of the carbon nanotube through the plate thickness. Draoui et al. [16] studied the static and dynamic response of sandwich plates with CNTRC face sheets and homogeneous core and sandwich plates with homogeneous face sheet and CNTRC core. Alibeigloo and Liew [17] employed a three-dimensional theory of elasticity to obtain the bending responses of simply supported FG-CNTRCs rectangular plates subjected to thermo-mechanical loads. Nonlinear cylindrical bending of simply supported FG-CNTRC plates in thermal environments was investigated by Bakhti et al. [18]. Zerouki et al. [19] have proposed a new exponential function of the volume fraction of carbon nanotubes (CNT) in conjunction with higher-order shear deformation theory in order to obtain the optimal CNT distribution on the bending behavior of CNTRC beams. Sobhy [20] presented a new analytical approach for bending response of functionally graded single-walled carbon nanotube (FG-CNT) reinforced plate resting on double-layered elastic foundations and subjected to uniform, linear, sinusoidal, or exponential distributed loadings; levy and Navier type's solutions are used to handle governing equations.

In contrast to reinforced single-layer CNTRC plates, multi-layers CNTRC plates have failure modes that are very different from a single layer, especially in a thermal environment, such as delamination failure due to the weakness of the layer interface zone under concentrated thermal stress. And this requires developing methods that can systematically study the behavior of this kind of composite structure. The First-order shear deformation plate's theory (FSDT) is a simple analytical solution to study the CNT laminated structures in which the transverse shear strains are assumed to be constant across the thickness direction so, shear correction factors (SCF) have to be incorporated to adjust the transverse shear stiffness. In this context, several studies have been presented. Zeverdejani and Beni [21] have investigated the buckling and free vibration behavior of polymeric laminate reinforced graphene sheets. Same authors [22] have studied the buckling and post-buckling behavior of Multi-layer rectangular laminated reinforced composite plates, perfect and defective graphene sheets are considered as reinforcement, various boundary conditions were taken into account. In both studies, the mechanical properties of the composite were calculated using molecular dynamics (MD) and the rule of mixture (MR). Kiani [23] presented a study on the free torsional vibration of a composite conical shell made of a polymeric matrix reinforced with carbon nanotube (CNTs); the mathematical formulation was based on the First-order shear deformation shell theory (FSDT), compatible with the Donnell kinematic assumptions to derive the motion equations of the shell. Long and Tung [24] studied buckling and post-buckling responses of sandwich plates reinforced by single-walled carbon nanotubes (CNT) resting on elastic foundations and subjected to uniform temperature rise, considering that the mechanical properties depend on temperature, the mathematical formulation was based on the first-order shear deformation theory taking into consideration geometrical nonlinearity and initial geometrical imperfection. Furthermore, the thermo-mechanical analysis of laminated and sandwich plates was reported by Han et al. [25] through a new enhanced first-order shear deformation theory, the latter was reached by considering the thermal transverse normal strain effect under the plane stress condition. It seems that the efficiency of FSDT is dependent on the SCF, which in turn depends on different parameters. To overcome the dependency of shear correction factors in FSDT theory, Higher-order shear deformation theory (HSDT) was developed in which the in-plane displacements are expanded as a higher-order function of thickness direction, making that the zero transverse shear stresses condition on the upper and lower surfaces of the plate is respected, which leads to a correct representation of transverse strain across the thickness coordinate without the need for any shear correction factors. Using various shear deformation plate theories, Daikh et al. [26] presented a study on the bending behavior of single-walled CNTRC laminated plates, a uniform distribution (UD), and three functionally graded types of reinforcement material distributions (FG) were inspected. Fazzolari et al. [27] presented the buckling response of composite plate using HSDT and the dynamic stiffness method. Khdeir and reddy [28] have studied the thermal stresses and deflections of cross-ply rectangular plates under various boundary conditions using the third-order plate's theory and levy approach to solve the governing equations. Zenkour [29] presented a unified shear deformable plate theory to investigate the thermo-elastic response of symmetric and anti-symmetric cross-ply laminated plates subjected to non-uniform thermal or thermo-mechanical loads. Shen [30] investigated the nonlinear bending of simply supported FG-CNTRCs under thermo-mechanical loading using higher-order shear deformation theory (HSDT) in conjunction with Von Karman nonlinearity. Bakhadda et al. [31] investigated the free vibration and bending behavior of SW-CNT reinforced composite plates embedded on Pasternak elastic foundation using new HSDT. Recently, Naik and Sayyad [32] presented a new fifth-order shear and normal deformation theory (quasi 3D) involving polynomial function in terms of thickness coordinates to the thermal analysis of laminated composite and sandwich plates. Although this mathematical model gives very satisfactory results, it contains a large number of unknown variables (09), which increases the computational time. Using a refined plate theory, Kaci et al. [33] studied the bending behavior of FG-CNTRC plates. Kamarian et al. [34] studied the thermal buckling of sandwich plates with composite face sheets in various boundary conditions, carbon nanotube CNTs were used to reinforce epoxy polymer which is used as face sheets. It reveals that the CNTs can increase the critical buckling temperature of sandwich plates by 22–36%. Likewise, the influence of temperature on the mechanical response of functionally graded plates is analyzed in various researches (see, e.g., Refs. [35-40]).

Among the effective methods used by the authors to study laminated FG-CNT structures is the finite element method, which can analyze complex geometric shapes. The following studies are based on this method to study the behavior of FG-CNT laminated structures. Pashmforoush [41] studied the impact of CNT on the damage modes of carbon fiber reinforced composites CFRC developed during transverse low velocity through the ABAQUS/Explicit environment. A cohesive surface element was used to simulate delamination mode. It is proved that the addition of CNT until a certain point can improve the damage performance of CFRC. Mehar and Panda [42] presented a theoretical study using a finite element formulation of Reddy's HSDT mid-plane kinematics to examine the influence of the multi-walled carbon nanotube reinforcement on the stiffness of the sandwich curved panel. The importance of this study is to use a laboratory experimentation to validate the analytical results obtained. A ten degree of freedom (DOFs) quasi 3-D shear deformation theory is formulated by Adhikari and Singh [43] to obtain the thermo-mechanical response of cross-ply and angle ply laminated FG-CNTRC plates, only the linear temperature gradient across the thickness of the plate is considered in this study. Akbas and Kocatürk [44] developed a 3-D brick finite element with eight-node to study the post-buckling behavior of FG beams subject to temperature loading, in which dependent-temperature material properties are considered. Akbas [45] investigated the thermal environment and dependent-temperature material properties' effect on the free-vibration of axially-functional graded materials beams. Finite element formulation based on Euler-Bernoulli beam element was utilized as a numerical solution of governing differential motion equations. A finite element formulation based on the first-order plate theory together with an exact closed-form solution has been presented by Reddy and Han [46] to investigate the effects of shear deformation and anisotropy on the behavior of multilayer composite plates subjected to thermal and mechanical loading. A C^0 nine-noded isoparametric shell element was developed by Ansari and Kumar [47-49] to account for bending and flexural analysis of CNT reinforced truncated, truncated rhombic cone, and the plate's composites structures. The mathematical formulation was based on Taylor's series up to third-degree of thickness direction and normal curvatures in membrane displacement. The rule of mixture was utilized to predict the material properties of the CNT reinforced composite. The static and dynamic behaviors of FG-CNT-reinforced rhombic laminate plates are also examined by the same isoperimetric shell finite element by Ansari et al. [50]. The success of this element motivates the authors to extend it to investigate: the free vibration analysis of laminated composite shells with cutouts and concentrated mass [51]; the Dynamic behavior of laminated composite skew shells with multiple cutouts and concentrated mass [52]; the free vibration behavior of opening Multi-layer and sandwich rhombic in conjunction with higher-order shear deformation theory [53]. The advantage of this FEM formulation is also simple to implement and can easily integrate into commercial software, and provide accurate results with fast processing. Furthermore, Akbas [54] studied the effect of large deflections caused by geometrically nonlinear of a fiber-reinforced composite cantilever beam subjected to point loads. Total Lagrangian approach to gather with Newton-Raphson iteration method was utilized to handle the nonlinear problem. The nonlinear bending of laminated composite beams in a Hygro-thermal environment was investigated by Akbas [55]. The finite element formulation was used within the first-order shear beam theory as a numerical solution of the problem. The dynamic characteristics and forced vibrations of a laminated composite beam and a composite fiber cantilever beam subjected to harmonic loading were investigated by Akbas [56, 57], respectively. Timoshenko's beam theory was employed with the Ritz method to solve the problem. Algebraic polynomials with trivial Ritz functions were also used. Newmark average acceleration method was used in the history of time. Recently, the buckling and post-buckling behavior of laminated FG-CNT reinforced composite plates subjected to uniform and parabolic loading using both FEA via Abaqus software and an analytical solution have presented by Nguyen et al. [58], Von Kármán's geometric nonlinearity was utilized to derive the governing equations.

Based on the above literature, it is clear that many attempts have been made to study the vibration, bending, and buckling behavior of FG-CNTRC with or without temperature dependent material properties using different methods. However, to the best of the author's knowledge, the effects of nonlinear and combined variation of temperature on the thermal bending of CNTRC cross-ply composite laminated plates are not reported yet. Hence, the authors aim through this paper to propose a new mathematical formulation based on new higher shear deformation plate theory (HSDT) for FG-CNTRC cross-ply composite laminated plates subjected to linear, nonlinear, and combined variation thermal loading through plate thickness considering two types of single walled carbon nanotubes distribution fibers namely uniform (UD) and functional graded (FG) distribution. This model is simple and contains only four unknown variables and therefore a reduced number of governing equations to resolve, making it suitable for time-consuming computation. In addition, the present investigation aims to achieve the effect of two types of CNT dispersion: UD and FG (FG-X, FG-O and FG-V), CNT volume fraction, thickness to side ratio, aspect ratio, and laminated composites structure, linear, nonlinear, and combined variation of temperature through plate thickness direction on the thermal bending responses of FG-CNTRC symmetric and anti-symmetric cross-ply composite laminated plates.

2. Formulation of FSDT for CNTRC Laminated Plate

2.1 Geometry and materials properties

Consider a CNT fiber-reinforced rectangular laminated plate of length a, width b and uniform thickness h (see Fig. 1). The plate composed of N orthotropic layers oriented at angles θ_1, θ_2,........,θ_N. The coordinate system is such that the mid-plane of the plate coincides with x-y plane, and z axis is normal to the middle plane. The upper surface of the plate (z = -*h*/2) is subjected to a sinusoidal thermal load *T*(*x*,*y*,*z*). The region of the plate in $(0:x,y,z)$ right handed Cartesian coordinate system is $0 \le x \le a;\ 0 \le y \le b;\ -h/2 \le z \le h/2$ (Fig. 1). Each layer of the considered plate is reinforced by single-walled carbon nanotubes. The bounding of SWCNT and matrix is taken to be perfect. Three configurations of functionally graded (FG), and uniformly distribution (UD) of SWCNT fibers over the thickness are considered, as shown in Fig. 1(b). $z_{(k)}$ and $z_{(k-1)}$ are the vertical positions of the bottom face and the top face of *k*th layer of CNTRC laminated plate. Volume fraction of several types of distributions of reinforcement material is expressed mathematically as:

$$\text{FG-X CNTRC laminated plate: } V_{cnt} = 2\frac{\left|2|z| - |z_{k-1} + z_k|\right|}{z_k - z_{k-1}} V_{cnt}^{*} \tag{1}$$

$$\text{FG-O CNTRC laminated plate: } V_{cnt} = 2\left(1 - \frac{\left|2|z| - |z_{k-1} + z_k|\right|}{z_k - z_{k-1}}\right) V_{cnt}^{*} \tag{2}$$

$$\text{FG-V CNTRC laminated plate: } V_{cnt} = 1 - \left(\frac{2z - z_k - z_{k-1}}{z_k - z_{k-1}}\right) V_{cnt}^{*} \tag{3}$$

$$\text{UD CNTRC laminated plate: } V_{cnt} = V_{cnt}^{*} \tag{4}$$

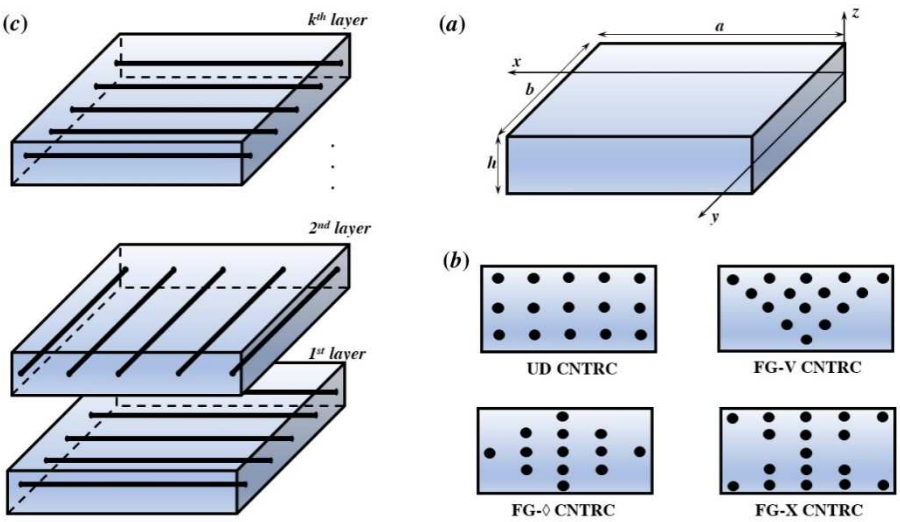

Fig. 1. Geometry and cross-sections of FG-CNTRC laminated plate.

Note that V_{cnt} is the volume fraction of the carbon nanotubes and V_{cnt}^{*} is a given volume fraction of CNTs, which can be calculated from the equation:

$$V_{cnt}^{*} = \frac{W_{cnt}}{W_{cnt} + (\rho_{cnt} / \rho_m)(1 - W_{cnt})} \tag{5}$$

where W_{cnt}, ρ_{cnt} and ρ_m are CNTs mass fraction, CNTs mass density and polymer matrix mass density, respectively.

The CNTRC laminate plate is made of k^{th} layers, having the same mechanical properties. Hence, the constitutive stress-strain relations are stated as:

$$\begin{Bmatrix} \sigma_x \\ \sigma_y \\ \tau_{yz} \\ \tau_{xz} \\ \tau_{xy} \end{Bmatrix}^{(k)} = \begin{bmatrix} \bar{Q}_{11}^k & \bar{Q}_{12}^k & 0 & 0 & 0 \\ \bar{Q}_{12}^k & \bar{Q}_{22}^k & 0 & 0 & 0 \\ 0 & 0 & \bar{Q}_{44}^k & 0 & 0 \\ 0 & 0 & 0 & \bar{Q}_{55}^k & 0 \\ 0 & 0 & 0 & 0 & \bar{Q}_{66}^k \end{bmatrix} \begin{Bmatrix} \varepsilon_x - \alpha_{11} T \\ \varepsilon_y - \alpha_{22} T \\ \gamma_{yz} \\ \gamma_{xz} \\ \gamma_{xy} \end{Bmatrix}^{(k)} \tag{6}$$

where the transformed material constants $\bar{Q}_{11}^k$ are expressed as [59]:

$$\begin{aligned} \bar{Q}_{11}^k &= Q_{11}\cos^4\theta_k + 2(Q_{12} + 2Q_{66})\sin^2\theta_k\cos^2\theta_k + Q_{22}\sin^4\theta_k \\ \bar{Q}_{12}^k &= (Q_{11} + Q_{12} - 4Q_{66})\sin^2\theta_k\cos^2\theta_k + Q_{12}(\sin^4\theta_k + \cos^4\theta_k) \\ \bar{Q}_{22}^k &= Q_{11}\sin^4\theta_k + 2(Q_{12} + 2Q_{66})\sin^2\theta_k\cos^2\theta_k + Q_{22}\cos^4\theta_k \\ \bar{Q}_{66}^k &= (Q_{11} + Q_{22} - 2Q_{12} - 2Q_{66})\sin^2\theta_k\cos^2\theta_k + Q_{66}(\sin^4\theta_k + \cos^4\theta_k) \\ \bar{Q}_{44}^k &= Q_{44}\cos^2\theta_k + Q_{55}\sin^2\theta_k \\ \bar{Q}_{55}^k &= Q_{55}\cos^2\theta_k + Q_{44}\sin^2\theta_k \end{aligned} \tag{7}$$

where θ_k is the lamination angle of k^{th} layer, and

$$\begin{aligned} &Q_{11} = \frac{E_{11}}{1 - \nu_{12}\nu_{21}},\ Q_{22} = \frac{E_{22}}{1 - \nu_{12}\nu_{21}},\ Q_{12} = \frac{\nu_{12}E_{12}}{1 - \nu_{12}\nu_{21}}. \\ &Q_{44} = G_{23},\ Q_{55} = G_{13},\ Q_{66} = G_{12} \end{aligned} \tag{8}$$

where E_{11}, E_{22}, G_{12}, ν_{12} and ν_{21} are the Young's modulus, shear modulus and Poisson's ratio across the plane directions (x, y), of the plate respectively. The effective material properties of the CNTRCs are obtained based on the rule of mixture as follows:

$$\begin{aligned} &E_{11} = \eta_1 V_{cnt} E_{11}^{cnt} + V_m E_m; \\ &\frac{\eta_2}{E_{22}} = \frac{V_{cnt}}{E_{22}^{cnt}} + \frac{V_m}{E_m}; \\ &\frac{\eta_3}{E_{12}} = \frac{V_{cnt}}{G_{12}^{cnt}} + \frac{V_m}{G_m} \end{aligned} \tag{9}$$

The subscripts *m* and *cnt* refer to the properties of polymer matrix and CNTs, respectively. The CNT efficiency parameters η_i (i=1, 2, 3) are given as:

$$\text{For } V_{cnt}^{*} = 0.11;\ \eta_1 = 0.149,\ \eta_2 = \eta_3 = 0.934$$

$$\text{For } V_{cnt}^{*} = 0.14;\ \eta_1 = 0.150,\ \eta_2 = \eta_3 = 0.941$$

$$\text{For } V_{cnt}^{*} = 0.17;\ \eta_1 = 0.149,\ \eta_2 = \eta_3 = 1.381$$

It is noticed that the sum of the volume fractions of the polymer and CNTs constituents equals to unity:

$$V_{cnt}^k + V_m^k = 1 \tag{10}$$

Poisson's ratio ν_{12} of *k* layer is dependent upon the position of the CNT fiber. So, it is expressed as the function of thickness coordinate of the plate as [60]:

$$\nu_{12} = V_{cnt}\nu_{12}^{cnt} + V_m \nu_m \tag{11}$$

The thermal expansion coefficient in the longitudinal and transverse direction of the laminated FG-CNTRC plate can be expressed as [13, 43]:

$$\alpha_{11} = V_{cnt}\alpha_{11}^{cnt} + V_m \alpha_m \tag{12}$$

$$\alpha_{22} = (1 + \nu_{12}^{cnt})V_{cnt}\alpha_{22}^{cnt} + (1 + \nu_m)V_m\alpha_m - \nu_{12}\alpha_{11} \tag{13}$$

where α_{11}^{cnt}, α_{22}^{cnt} and α_m are the in-plane and transverse thermal expansion coefficients of CNT fibers and polymer matrix respectively.

2.2 Kinematics of the Plates

In this section the high-order shear deformation plate model HSDT is proposed for modeling CNTRC cross-ply laminated plate, based on the conventional HSDT [46] which has five structural unknown as follows:

$$
\begin{aligned}
u(x,y,z) &= u_0 - z\frac{\partial w_0(x,y)}{\partial x} + f(z)\varphi_x(x,y) \\
v(x,y,z) &= v_0 - z\frac{\partial w_0(x,y)}{\partial y} + f(z)\varphi_y(x,y) \\
w_0(x,y,z) &= w_0(x,y)
\end{aligned}
\tag{14}
$$

where (u_0, v_0, w_0) and $(\varphi_x,\ \varphi_y)$ are displacement components along the (x, y) directions, and rotations of transverse normal's about the x and y axes of the mid-plane of the plate, respectively. In order to diminish the unknowns of conventional HSDT, additional simplifying assumptions are considered, supposing that $\varphi_x = \int \theta(x,y)dx$ and $\varphi_y = \int \theta(x,y)dy$ [61-63]. The displacement field can be written as follows:

$$
\begin{aligned}
u(x,y,z) &= u_0 - z\frac{\partial w_0(x,y)}{\partial x} + k_1 f(z)\int \theta(x,y)dx \\
v(x,y,z) &= v_0 - z\frac{\partial w_0(x,y)}{\partial y} + k_2 f(z)\int \theta(x,y)dy \\
w_0(x,y,z) &= w_0(x,y)
\end{aligned}
\tag{15}
$$

The integrals defined in Eq. (15) shall be resolved by a Navier type method and the displacement fields can be rewritten as a new and simple form to reduce unknowns as:

$$
\begin{aligned}
u(x,y,z) &= u_0 - z\frac{\partial w_0(x,y)}{\partial x} - f(z)\frac{\partial \theta}{\partial x} \\
v(x,y,z) &= v_0 - z\frac{\partial w_0(x,y)}{\partial y} - f(z)\frac{\partial \theta}{\partial y} \\
w_0(x,y,z) &= w_0(x,y)
\end{aligned}
\tag{16}
$$

where $f(z)$ is the shape function determining the distribution of the transverse shear strains and stresses along the thickness of CNTRC laminated plate, and is given as:

$$
f(z) = \frac{z\cosh(\frac{\pi}{2}) - \frac{\pi}{h}\sinh(\frac{\pi}{2}z)}{\cosh(\frac{\pi}{2}) - 1}
\tag{17}
$$

The deformation components associated with the above displacements can be expressed as

$$
\begin{aligned}
&\begin{Bmatrix} \varepsilon_{xx} \\ \varepsilon_{yy} \\ \gamma_{xy} \end{Bmatrix} = \begin{Bmatrix} \varepsilon_{xx}^0 \\ \varepsilon_{yy}^0 \\ \gamma_{xy}^0 \end{Bmatrix} + z\begin{Bmatrix} k_x^b \\ k_y^b \\ k_{xy}^b \end{Bmatrix} + f(z)\begin{Bmatrix} k_x^s \\ k_y^s \\ k_{xy}^s \end{Bmatrix} \\
&\begin{Bmatrix} \gamma_{yz} \\ \gamma_{xz} \end{Bmatrix} = g(z)\begin{Bmatrix} \gamma_{yz}^s \\ \gamma_{xz}^s \end{Bmatrix},\ g(z) = \frac{df(z)}{dz}
\end{aligned}
\tag{18}
$$

where

$$
\begin{aligned}
&\begin{Bmatrix} \varepsilon_{xx}^0 \\ \varepsilon_{yy}^0 \\ \gamma_{xy}^0 \end{Bmatrix} = \begin{Bmatrix} \dfrac{\partial u_0}{\partial x} \\ \dfrac{\partial v_0}{\partial y} \\ \dfrac{\partial u_0}{\partial y} + \dfrac{\partial v_0}{\partial x} \end{Bmatrix};\ \begin{Bmatrix} k_x^b \\ k_y^b \\ k_{xy}^b \end{Bmatrix} = -\begin{Bmatrix} \dfrac{\partial^2 w_0}{\partial x^2} \\ \dfrac{\partial^2 w_0}{\partial y^2} \\ 2\dfrac{\partial^2 w_0}{\partial x \partial y} \end{Bmatrix}; \\
&\begin{Bmatrix} k_x^s \\ k_y^s \\ k_{xy}^s \end{Bmatrix} = -\begin{Bmatrix} \dfrac{\partial^2 \theta}{\partial x^2} \\ \dfrac{\partial^2 \theta}{\partial y^2} \\ 2\dfrac{\partial^2 \theta}{\partial x \partial y} \end{Bmatrix};\ \begin{Bmatrix} \gamma_{yz}^s \\ \gamma_{xz}^s \end{Bmatrix} = -\begin{Bmatrix} \dfrac{\partial \theta}{\partial x} \\ \dfrac{\partial \theta}{\partial y} \end{Bmatrix}.
\end{aligned}
\tag{19}
$$

3. Equations of Motion

The governing equations of equilibrium can be derived by using the principle of virtual displacements. The principle of virtual work in the present case yields:

$$
\int_v (\sigma_{xx}^k \delta\varepsilon_{xx} + \sigma_{yy}^k \delta\varepsilon_{yy} + \tau_{xy}^k \delta\gamma_{xy} + \tau_{xz}^k \delta\gamma_{xz} + \tau_{yz}^k \delta\gamma_{yz})dV = 0
\tag{20}
$$

Substituting Eqs. (6) and (18) into Eq. (20) and integrating through the thickness of the plate, Eq. (20) can be rewritten as

$$
\int_A (N_x \delta\varepsilon_{xx}^0 + N_y \delta\varepsilon_{yy}^0 + N_{xy}\delta\gamma_{xy}^0 + M_x^b \delta k_x^b + M_y^b \delta k_y^b + M_{xy}^b \delta k_{xy}^b + M_x^s \delta k_x^s + M_y^s \delta k_y^s + M_{xy}^s \delta k_{xy}^s + Q_{xz}\delta\gamma_{xz}^s + Q_{yz}\delta\gamma_{yz}^s)\ dA = 0
\tag{21}
$$

where A is the top surface and (N_x, N_y, N_{xy}) indicate the total in-plane force resultants, (M_x^b, M_y^b, M_{xy}^b) are the stress couples, (M_x^s, M_y^s, M_{xy}^s) and (Q_{xz}, Q_{yz}) are the additional stress couples and transverse shear stress resultants, respectively, and they are expressed as:

$$\begin{Bmatrix} N_x \\ N_y \\ N_{xy} \end{Bmatrix} = \sum_{k-1}^{n} \int_{z_{k-1}}^{z_k} \begin{Bmatrix} \sigma_{xx} \\ \sigma_{yy} \\ \tau_{xy} \end{Bmatrix}^k dz \tag{22}$$

$$\begin{Bmatrix} M_x^b \\ M_y^b \\ M_{xy}^b \end{Bmatrix} = \sum_{k-1}^{n} \int_{z_{k-1}}^{z_k} \begin{Bmatrix} \sigma_{xx} \\ \sigma_{yy} \\ \tau_{xy} \end{Bmatrix}^k z\, dz \tag{23}$$

$$\begin{Bmatrix} M_x^s \\ M_y^s \\ M_{xy}^s \end{Bmatrix} = \sum_{k-1}^{n} \int_{z_{k-1}}^{z_k} \begin{Bmatrix} \sigma_{xx} \\ \sigma_{yy} \\ \tau_{xy} \end{Bmatrix}^k f(z)\, dz \tag{24}$$

$$\begin{Bmatrix} Q_{yz} \\ Q_{xz} \end{Bmatrix} = \sum_{k-1}^{n} \int_{z_{k-1}}^{z_k} \begin{Bmatrix} \tau_{yz} \\ \tau_{xz} \end{Bmatrix}^k g(z)\, dz \tag{25}$$

Using Eq. (6) in Eqs (22)-(25), the stress resultants including thermal ones of the CNTRC laminated plate can be related to the total strains by:

$$\begin{Bmatrix} \{N\} \\ \{M^b\} \\ \{M^s\} \end{Bmatrix} = \begin{bmatrix} [A] & [B] & [B^s] \\ [B] & [D] & [D^s] \\ [B^s] & [D^s] & [H^s] \end{bmatrix} \begin{Bmatrix} \{\varepsilon^0\} \\ \{k^b\} \\ \{k^s\} \end{Bmatrix} - \begin{Bmatrix} \{N^T\} \\ \{M^{bT}\} \\ \{M^{sT}\} \end{Bmatrix}$$
$$\begin{Bmatrix} Q_{yz} \\ Q_{xz} \end{Bmatrix} = \begin{bmatrix} A_{44} & 0 \\ 0 & A_{55} \end{bmatrix} \begin{Bmatrix} \gamma_{yz}^s \\ \gamma_{xz}^s \end{Bmatrix} \tag{26}$$

The following definitions are used in (26)

$$\{N\} = \{N_x, N_y, N_{xy}\}^t, \{M^b\} = \{M_x^b, M_y^b, M_{xy}^b\}^t, \{M^s\} = \{M_x^s, M_y^s, M_{xy}^s\}^t$$
$$\{N^T\} = \{N_x^T, N_y^T, 0\}^t,\ \{M^{bT}\} = \{M_x^{bT}, M_y^{bT}, 0\}^t,\ \{M^{sT}\} = \{M_x^{sT}, M_y^{sT}, 0\}^t \tag{27}$$
$$\{\varepsilon^0\} = \{\varepsilon_x^0, \varepsilon_y^0, \gamma_{xy}^0\}, \{k^b\} = \{k_x^b, k_y^b, k_{xy}^b\}, \{k^b\} = \{k_x^s, k_y^s, k_{xy}^s\}$$

Here A_{ij}, B_{ij},..., H_{ij} are the composite plate stiffness, given as

$$\{A_{ij}, B_{ij}, B_{ij}^s, D_{ij}, D_{ij}^s, H_{ij}^s\} = \sum_{k=1}^{n} \int_{z_{(k-1)}}^{z_{(k)}} \bar{Q}_{11}^k \{1, z, f(z), z^2, zf(z), f^2(z)\} dz;$$
$$A_{cc}^s = \sum_{k=1}^{n} \int_{z_{(k-1)}}^{z_{(k)}} \bar{Q}_{cc}^k [g(z)]^2 dz.\ (i,j=1,2,6, c=4,5) \tag{28}$$

The stress and moment resultants $N_x^T, N_y^T, M_x^{bT}, M_y^{bT}, M_x^{sT}$ and M_y^{sT} due to thermal loading are defined by

$$\begin{Bmatrix} N_x^T \\ M_x^{bT} \\ M_x^{sT} \end{Bmatrix} = \sum_{k=1}^{n} \int_{z_{(k-1)}}^{z_{(k)}} (\bar{Q}_{11}^k \alpha_{11} + \bar{Q}_{12}^k \alpha_{22}) T \begin{Bmatrix} 1 \\ z \\ f(z) \end{Bmatrix} dz \tag{29-a}$$

$$\begin{Bmatrix} N_x^T \\ M_x^{bT} \\ M_x^{sT} \end{Bmatrix} = \sum_{k=1}^{n} \int_{z_{(k-1)}}^{z_{(k)}} (\bar{Q}_{12}^k \alpha_{11} + \bar{Q}_{22}^k \alpha_{22}) T \begin{Bmatrix} 1 \\ z \\ f(z) \end{Bmatrix} dz \tag{29-b}$$

The form of the temperature field change across the plate thickness is the result of the solution of a heat conduction problem. So, the temperature field, which considers linear, nonlinear, and combined temperature, is assumed to be varied through the thickness as [29, 39]

$$T(x,y,z) = t_1(x,y) + \frac{z}{h} t_2(x,y) + \frac{f(z)}{h} t_3(x,y) \tag{30-a}$$

The temperature field which takes into account only the linear variation through the thickness is such [43]

$$T(x,y,z) = t_1(x,y) + \frac{z}{h} t_2(x,y) \tag{30-b}$$

where t_1 t_2 and t_3 are thermal loads. The governing equations of equilibrium can be derived from Eq. (20) by integrating the displacement gradients by parts and setting the coefficients of δu_0 , δv_0 , δw_0 and $\delta\theta$ zero separately. Thus one can obtain the equilibrium equations associated with the present shear deformation theory

$$\begin{aligned}
&\delta u_0:\frac{\partial N_x}{\partial x}+\frac{\partial N_{xy}}{\partial y}=0\\
&\delta v_0:\frac{\partial N_{xy}}{\partial x}+\frac{\partial N_y}{\partial y}=0\\
&\delta w_0:\frac{\partial^2 M_x^b}{\partial x^2}+2\frac{\partial^2 M_{xy}^b}{\partial x\partial y}+\frac{\partial^2 M_y^b}{\partial y^2}=0\\
&\delta\theta:\frac{\partial^2 M_x^s}{\partial x^2}+2\frac{\partial^2 M_{xy}^s}{\partial x\partial y}+\frac{\partial^2 M_y^s}{\partial y^2}+\frac{\partial Q_{xz}}{\partial x}+\frac{\partial Q_{yz}}{\partial y}=0
\end{aligned}\tag{31}$$

4. Analytical Solutions

The current analysis is focused on cross-ply CNTRC laminated plate subjected to simply-supported edge conditions. These conditions are given by

$$\begin{aligned}
&v_0=w_0=\frac{\partial\theta}{\partial x}=N_x=M_x^b=M_x^s=0 \text{ at } x=0,a;\\
&u_0=w_0=\frac{\partial\theta}{\partial x}=N_y=M_y^b=M_y^s=0 \text{ at } y=0,b.
\end{aligned}\tag{32}$$

The solutions that satisfy the above boundary conditions are given as

$$\begin{Bmatrix}u_0(x,y)\\ v_0(x,y)\\ w_0(x,y)\\ \theta(x,y)\end{Bmatrix}=\sum_{m=1}^{\infty}\sum_{n=1}^{\infty}\begin{Bmatrix}U_{mn}\cos(\lambda x)\sin(\mu y)\\ V_{mn}\sin(\lambda x)\cos(\mu y)\\ W_{mn}\sin(\lambda x)\sin(\mu y)\\ \psi_{mn}\sin(\lambda x)\sin(\mu y)\end{Bmatrix}\tag{33}$$

where $\lambda=m\pi/a$, $\mu=n\pi/b$ and U_{mn} , V_{mn} , W_{mn} and Ψ_{mn} are unknown arbitrary parameters. To solve this problem, Navier presented the transverse temperature loads T_1 , T_2 and T_3 in the form of a double trigonometric series as

$$\begin{Bmatrix}t_1\\ t_2\\ t_3\end{Bmatrix}=\sum_{m=1}^{\infty}\sum_{n=1}^{\infty}\begin{Bmatrix}T_1\\ T_2\\ T_3\end{Bmatrix}\sin(\lambda x)\sin(\mu y\tag{34}$$

Substitution of Eqs. (33)- (34), into Eq. (31), and the use of Eqs. (26)- (29) give

$$[L]\{\Lambda\}=\{F\}\tag{35}$$

The column $\{\Lambda\}$ and the elements L_{ij} symmetric matrix $[L]$ are obtained as

$$\{\Lambda\}=\{U,V,W,\psi\}^t\tag{36}$$

$$\begin{aligned}
&L_{11}=A_{11}\lambda^2+A_{66}\mu^2\\
&L_{12}=(A_{12}+A_{66})\lambda\mu\\
&L_{13}=-B_{11}\lambda^3-(B_{12}+2B_{66})\lambda\mu^2\\
&L_{14}=-B_{11}^s\lambda^3-(B_{12}^s+2B_{66}^s)\lambda\mu^2\\
&L_{22}=A_{22}\mu^2+A_{66}\lambda^2\\
&L_{23}=-B_{22}\mu^3-(B_{12}+2B_{66})\lambda^2\mu\\
&L_{24}=-B_{22}^s\mu^3-(B_{12}^s+2B_{66}^s)\lambda^2\mu\\
&L_{33}=D_{11}\lambda^4+D_{22}\mu^4+2(D_{12}+2D_{66})\lambda^2\mu^2\\
&L_{34}=D_{11}^s\lambda^4+D_{22}^s\mu^4+2(D_{12}^s+2D_{66}^s)\lambda^2\mu^2\\
&L_{44}=H_{11}^s\lambda^4+H_{22}^s\mu^4+2(H_{12}^s+2H_{66}^s)\lambda^2\mu^2+A_{55}^s\lambda^2+A_{44}^s\mu^2
\end{aligned}\tag{37}$$

The components of the generalized thermal force vector are given by

$$\{F\}=\begin{Bmatrix}\lambda\left(A_1^TT_1+B_1^TT_2+C_1^TT_3\right)\\ \mu\left(A_2^TT_1+B_2^TT_2+C_2^TT_3\right)\\ \lambda^2\left(B_1^TT_1+C_1^TT_2+D_1^{sT}T_3\right)+\mu^2\left(B_2^TT_2+C_2^TT_2+D_2^{sT}T_3\right)\\ \lambda^2\left(B_1^TT_1+D_1^{sT}T_2+H_1^{sT}T_3\right)+\mu^2\left(B_2^TT_2+D_2^{sT}T_2+H_2^{sT}T_3\right)\end{Bmatrix}\tag{38}$$

where

$$\begin{Bmatrix} A_i^T \\ B_i^T \\ C_i^T \end{Bmatrix} = \sum_{k=1}^{n} \int_{z_{(k-1)}}^{z_{(k)}} (\bar{Q}_{i1}^k \alpha_{11} + \bar{Q}_{i2}^k \alpha_{22}) \begin{Bmatrix} 1 \\ \bar{z} \\ \bar{z}^2 \end{Bmatrix} dz, (i = 1,2)$$
$$\begin{Bmatrix} B_i^{sT} \\ D_i^{sT} \\ H_i^{sT} \end{Bmatrix} = \sum_{k=1}^{n} \int_{z_{(k-1)}}^{z_{(k)}} (\bar{Q}_{i1}^k \alpha_{11} + \bar{Q}_{i2}^k \alpha_{22}) \bar{f}(z) \begin{Bmatrix} 1 \\ \bar{z} \\ \bar{f}(z) \end{Bmatrix} dz, (i = 1,2) \tag{39-a}$$

$$\bar{z} = \frac{z}{h}$$
$$\bar{f}(z) = \frac{f(z)}{h} \tag{39-b}$$

5. Numerical Results and Discussion

5.1 Results validation

In this section we present through many examples the accuracy of present solution to evaluate the bending behavior of CNTRC symmetric and anti-symmetric cross-ply laminated plate's subjects to sinusoidal thermal loading. First, three-ply and four-ply rectangular cross-ply plates ($a = 10h$) with layers of equal thickness and subjected to sinusoidal temperature field linearly distributed through the thickness ($T_3 = 0$) studied by Zenkour [29] are considered for comparison. The lamina properties are assumed to be

$$E_1 = 25E_2;\ G_{12}=G_{13}=0.5E_2;\ G_{23}=0.2E_2;\ \nu_{12}=0.25;\ \alpha_2=3\alpha_1$$

The dimensionless displacements $\tilde{w}$ and the dimensionless in plane shear stress $\tilde{\tau}_{xy}$ are presented in Table 1 for cross-layers [0°/90°/90°/0°] laminated plates using present higher order displacement model with four unknown. While in Table 2 the deflections comparison $\tilde{w}$ is made for three-layer rectangular ($a = 10h$) cross-ply [0°/90°/0°] laminated plates. For a comparison purpose, the following dimensionless forms are used

$$\tilde{w}=10\frac{h}{\alpha_1 T_1 a^2} w(\frac{a}{2},\frac{b}{2})$$
$$\tilde{\tau}_{xy}=\frac{1}{\alpha_1 T_1 a^2} w(0,0,-\frac{h}{2}) \tag{40}$$

Table 1. Comparison between present model results and Zenkour [29] of dimensionless deflection $\tilde{w}$ and dimensionless shear in plane shear stress $\tilde{\tau}_{xy}$ for cross-ply [0°/90°/90°/0°] rectangular laminated plates

Theory	$\tilde{w}$			$\tilde{\tau}_{xy}$		
	a/b					
	0.5	1	2	0.5	1	2
SPT	1.21922	1.36011	0.74845	0.31685	0.66070	0.75813
HPT	1.21780	1.35812	0.64875	0.31691	0.66033	0.75828
FPT	1.20144	1.33206	0.75269	0.32094	0.65734	0.76015
CPT	1.14339	1.24451	0.75743	0.28212	0.61414	0.74755
Present	**1.21860**	**1.35930**	**0.74860**	**0.31690**	**0.66050**	**0.75820**

Table 2. Comparison between present model results and Zenkour [29] of dimensionless deflection $\tilde{w}$ for cross-ply [0°/90°/0°] rectangular laminated plates

a/h	Theory	$\tilde{w}$				
		a/b				
		1/3	1/2	1	1.5	2
	Exact	1.0998	1.1535	1.2224	1.0157	0.7355
	FPT	1.0998	1.1535	1.2224	1.0157	0.7355
5	HPT	1.1073	1.1689	1.2452	1.0169	0.7237
	SPT	1.1081	1.1704	1.2472	1.0167	0.7225
	Present	**1.1072**	**1.1689**	**1.2452**	**1.0169**	**0.7237**
	Exact	1.0619	1.0795	1.1058	0.9883	0.7601
	FPT	1.0619	1.0795	1.1058	0.9883	0.7601
0	HPT	1.0625	1.0808	1.1087	0.9892	0.7583
	SPT	1.0626	1.0810	1.1090	0.9893	0.7581
	Present	**1.0625**	**1.0808**	**1.1087**	**0.9892**	**0.7583**
	Exact	1.0593	1.0741	1.0949	0.9847	0.7643
	FPT	1.0593	1.0741	1.0949	0.9847	0.7643
100	HPT	1.0593	1.0741	1.0950	0.9847	0.7642
	SPT	1.0593	1.0741	1.0950	0.9847	0.7642
	Present	**1.0593**	**1.0741**	**1.0950**	**0.9847**	**0.7642**

From the Tables 1- 2, we observe very satisfactory results given by the current model, both for the calculation of dimensionless displacements $\bar{w}$ as well as dimensionless in-plane shear stress $\bar{\tau}_{xy}$ considering all values of a/b ratio for cross-layers [0°/90°/90°/0°] and [0°/90°/0°] laminated plates. It can be also noted that the current model yields results that are fully consistent with the HSDT model which contains five unknowns provided by Zenkour [29].

Secondly, in Table .3 we present the comparison between present model results and Adhikari and Singh [43] of dimensionless $\bar{w}$ deflection for CNTRC cross-ply [0°/90°/0°] square $(a/b=1)$ laminated plates. Adhikari and Singh [43] have studied thermo-elastic behavior of CNTRC laminated plate considering PmPV (Polymer) as the matrix and the armchair (10,10) SWCNTs to reinforce the polymeric matrix, in which elastic material characteristics of the two constituents are:

$$\nu^m = 0.34;\ \alpha^m = 45.10^{-6}/K;\ E^m = 2.1Gpa.$$
$$\nu_{12} = 0.175;\ \alpha_{11}^{cnt} = 3.4584.10^{-6}/K;\ \alpha_{22}^{cnt} = 5.1682.10^{-6}/K;\ E_{11}^{cnt} = 5.6466\text{TPa}; E_{22}^{cnt} = 7.080\ \text{TPa};$$
$$G_{12}^{cnt} = G_{13}^{cnt} = G_{23}^{cnt} = 1.9445\ \text{TPa}$$

In this case of CNTRC laminated plates the normalized transverse displacement and normalized stresses are presented with the following dimensionless forms

$$\begin{aligned}
&\bar{w} = \frac{10h}{\alpha^m T_2 a^2} w\left(\frac{a}{2},\frac{b}{2}\right)\\
&\bar{\sigma}_{xx} = \frac{10^3}{\alpha^m T_2 E_{22}^{cnt}} \sigma_{xx}\left(\frac{a}{2},\frac{b}{2},\frac{h}{2}\right)\\
&\bar{\sigma}_{yy} = \frac{10^3}{\alpha^m T_2 E_{22}^{cnt}} \sigma_{yy}\left(\frac{a}{2},\frac{b}{2},\frac{h}{6}\right)\\
&\bar{\tau}_{xy} = \frac{10^3}{\alpha^m T_2 E_{22}^{cnt}} \tau_{xy}\left(0,0,-\frac{h}{2}\right)\\
&\bar{\tau}_{xz} = \frac{10^3}{\alpha^m T_2 E_{22}^{cnt}} \tau_{xz}\left(0,\frac{b}{2},0\right)\\
&\bar{\tau}_{yz} = \frac{10^3}{\alpha^m T_2 E_{22}^{cnt}} \tau_{xz}\left(\frac{a}{2},0,0\right)
\end{aligned} \tag{41}$$

The results summarized in Table 3 also illustrate the significant convergence between the current model and the FEM model of Adhikari and Singh [43]. Whereas, the percentage error between the two models, which was calculated as follows: $\text{Diff} = |(\text{FEM-Present})/\text{FEM}|$ does not exceed 0.5634% as the maximum estimate error, considering all the values of side to thickness a/h ratios for CNTRC plates.

Table 3. Comparison between present model results and Adhikari and Singh [43] of dimensionless $\bar{w}$ deflection for CNTRC cross-ply [0°/90°/0°] square laminated plates

			$a/h=5$	$a/h=10$	$a/h=50$	$a/h=100$
$V_{cnt}^{*}=0.11$	UD	FEM	0.8538	0.8742	0.8840	0.8844
		Present	0.8539	0.8723	0.8816	0.8820
		Diff %	**0.0117**	**0.2173**	**0.2715**	**0.2714**
	FG-X	FEM	0.8208	0.8405	0.8502	0.8505
		Present	0.8195	0.8384	0.8478	0.8482
		Diff %	**0.1584**	**0.2499**	**0.2823**	**0.2704**
	FG-O	FEM	0.8322	0.8486	0.8563	0.8565
		Present	0.8277	0.8440	0.8520	0.8522
		Diff %	**0.5407**	**0.5421**	**0.5022**	**0.5020**
	FG-V	FEM	0.8243	0.8438	0.8528	0.8532
		Present	0.8217	0.8410	0.8502	0.8506
		Diff %	**0.3154**	**0.3318**	**0.3049**	**0.3047**
$V_{cnt}^{*}=0.14$	UD	FEM	0.8320	0.8514	0.8610	0.8613
		Present	0.8342	0.8508	0.8596	0.8599
		Diff %	**0.2644**	**0.0705**	**0.1626**	**0.1625**
	FG-X	FEM	0.7855	0.8058	0.8162	0.8166
		Present	0.7844	0.8049	0.8151	0.8155
		Diff %	**0.1400**	**0.1117**	**0.1348**	**0.1347**
	FG-O	FEM	0.8069	0.8190	0.8249	0.8251
		Present	0.8052	0.8160	0.8217	0.8220
		Diff %	**0.2107**	**0.3663**	**0.3879**	**0.3757**
	FG-V	FEM	0.7941	0.8118	0.8203	0.8206
		Present	0.7921	0.8104	0.8191	0.8203
		Diff %	**0.2519**	**0.1725**	**0.1463**	**0.0366**
$V_{cnt}^{*}=0.17$	UD	FEM	0.8011	0.8199	0.8289	0.8293
		Present	0.8022	0.8188	0.8271	0.8274
		Diff %	**0.1373**	**0.1342**	**0.2172**	**0.2291**
	FG-X	FEM	0.7457	0.7655	0.7751	0.7755
		Present	0.7434	0.7637	0.7733	0.7737
		Diff %	**0.3084**	**0.2351**	**0.2322**	**0.2321**
	FG-O	FEM	0.7708	0.7810	0.7859	0.7860
		Present	0.7670	0.7766	0.7816	0.7818
		Diff %	**0.4930**	**0.5634**	**0.5471**	**0.5344**
	FG-V	FEM	0.7567	0.7728	0.7803	0.7805
		Present	0.7528	0.7704	0.7784	0.7786
		Diff %	**0.5154**	**0.3106**	**0.2435**	**0.2434**

Table 4. Dimensionless stresses of simply supported FG-CNTRC cross-ply [0°/90°/0°] rectangular laminated plates under linear sinusoidal temperature distribution ($T_3 = 0$) with $V_{cnt}^{*} = 0.11$

V_{cnt}^{*}		a/h	$\bar{\sigma}_{xx}$	$\bar{\sigma}_{yy}$	$\bar{\tau}_{yz}$	$\bar{\tau}_{xz}$	$\bar{\tau}_{xy}$
0.11	UD	5	-0.1911	-2.0043	-0.0073	-0.0077	0.0980
		10	-0.1893	-2.0023	-0.0053	-0.0054	0.1000
		50	-0.1886	-2.0012	-0.0012	-0.0012	0.1011
		100	-0.1886	-2.0011	-0.0006	-0.0006	0.1011
	FG-X	5	0.5430	-3.6184	-0.0048	-0.0073	0.1078
		10	0.5381	-3.6165	-0.0039	-0.0050	0.1098
		50	0.5329	-3.6154	-0.0010	-0.0012	0.1109
		100	0.5327	-3.6153	-0.0005	-0.0006	0.1109
	FG-O	5	-0.0377	-0.0178	-0.0085	-0.0073	0.0842
		10	-0.0357	-0.0157	-0.0055	-0.0049	0.0861
		50	-0.0348	-0.0147	-0.0012	-0.0011	0.0869
		100	-0.0348	-0.0147	-0.0006	-0.0006	0.0869
	FG-V	5	-0.0372	-3.6185	-0.0057	-0.0077	0.1078
		10	-0.0353	-3.6160	-0.0042	-0.0052	0.1098
		50	-0.0343	-3.6147	-0.0010	-0.0012	0.1108
		100	-0.0342	-3.6147	-0.0005	-0.0006	0.1108

Table 5. Dimensionless stresses of simply supported FG-CNTRC cross-ply [0°/90°/0°] rectangular laminated plates under linear sinusoidal temperature distribution ($T_3 = 0$) with $V_{cnt}^{*} = 0.14$

V_{cnt}^{*}		a/h	$\bar{\sigma}_{xx}$	$\bar{\sigma}_{yy}$	$\bar{\tau}_{yz}$	$\bar{\tau}_{xz}$	$\bar{\tau}_{xy}$
0.14	UD	5	-0.1955	-2.4996	-0.0067	-0.0072	0.0998
		10	-0.1912	-2.4977	-0.0050	-0.0052	0.1017
		50	-0.1894	-2.4966	-0.0012	-0.0012	0.1027
		100	-0.1893	-2.4966	-0.0006	-0.0006	0.1028
	FG-X	5	1.0701	-4.3632	-0.0038	-0.0077	0.1131
		10	1.0746	-4.3613	-0.0035	-0.0054	0.1152
		50	1.0720	-4.3601	-0.0009	-0.0013	0.1164
		100	1.0719	-3.7496	-0.0005	-0.0006	0.1164
	FG-O	5	-0.0437	-0.0190	-0.0080	-0.0054	0.0824
		10	-0.0422	-0.0173	-0.0052	-0.0039	0.0838
		50	-0.0415	-0.0165	-0.0012	-0.0009	0.0845
		100	-0.0415	-0.0165	-0.0006	-0.0004	0.0845
	FG-V	5	-0.0433	-4.3624	-0.0044	-0.0074	0.1133
		10	-0.0415	-4.3601	-0.0035	-0.0050	0.1152
		50	-0.0406	-4.3589	-0.0009	-0.0011	0.1162
		100	-0.0406	-5.2645	-0.0004	-0.0006	0.1163

Table 6. Dimensionless stresses of simply supported FG-CNTRC cross-ply [0°/90°/0°] rectangular laminated plates under linear sinusoidal temperature distribution ($T_3 = 0$) with $V_{cnt}^{*} = 0.17$

V_{cnt}^{*}		a/h	$\bar{\sigma}_{xx}$	$\bar{\sigma}_{yy}$	$\bar{\tau}_{yz}$	$\bar{\tau}_{xz}$	$\bar{\tau}_{xy}$
0.17	UD	5	-0.2774	-2.9172	-0.0103	-0.0110	0.1459
		10	-0.2750	-2.9142	-0.0074	-0.0076	0.1488
		50	-0.2743	-2.9127	-0.0017	-0.0017	0.1503
		100	-0.2743	-2.9126	-0.0009	-0.0009	0.1504
	FG-X	5	1.5859	-4.9065	-0.0057	-0.0111	0.1716
		10	1.5849	-4.9034	-0.0049	-0.0075	0.1749
		50	1.5792	-4.9016	-0.0012	-0.0017	0.1767
		100	1.5789	-4.9015	-0.0006	-0.0009	0.1768
	FG-O	5	-0.0623	-0.0060	-0.0120	-0.0079	0.1151
		10	-0.0603	-0.0036	-0.0076	-0.0055	0.1170
		50	-0.0593	-0.0025	-0.0017	-0.0012	0.1179
		100	-0.0592	-0.0025	-0.0008	-0.0006	0.1179
	FG-V	5	-0.0619	-4.9045	-0.0064	-0.0108	0.1721
		10	-0.0594	-4.9010	-0.0049	-0.0070	0.1750
		50	-0.0581	-4.8992	-0.0012	-0.0016	0.1764
		100	-0.0581	-4.8992	-0.0006	-0.0008	0.1765

Finally, for every useful purpose of research, we are shown in Tables 4,5 and 6 the dimensionless stresses of simply supported rectangular CNTRC cross-ply [0°/90°/0°] rectangular laminated plates under linear sinusoidal temperature distribution ($T_3 = 0$) for different values of CNTs volume fraction, 0.11, 0.14, 0.17 respectively. From these tables, it becomes clear that increasing CNT volume fraction lead to increasing of thermal stresses intensities. We can explain this recorded increasing to the good thermal and mechanical properties of carbon nanotube fibers. It is also clear that the FG-X CNTRC laminated plates give the largest thermal stress intensities.

5.2 Parametric studies

Based on the comparison study, the new developed higher order model of FG-CNTRC plate is extended to show the effect of different geometrical and material parameters on the bending of CNTRC symmetric and anti-symmetric cross-ply laminated plates under temperature loading. In general, the responses are analyzed for four grading configurations of FG-CNTRC plate (UD, FG-X, FG-O and FG-V), $a/h = 10$, $a/b = 1$ and $T_2 = 100$ throughout the analysis unless otherwise stated. For the numerical results purpose, the thickness of the composite plate is taken as $h = 1$ mm throughout the analysis. Many new numerical examples have been solved for the different design parameters (side to thickness ratio, aspect ratios, temperature load, CNT grading configurations and CNT volume fractions). The results of the parametric study are illustrated as follows.

Figure 2 shows transverse displacement $\bar{w}$ of rectangular simply supported FG-CNTRC plates subject to linear temperature distribution as function of aspect ratio a/b for different laminated composites structure and CNT graded configuration. From this figure there is a sharp increase in defection values for a small increase in the values of the a/b ratio until reaching the unit value (square plate), subsequently the transverse displacement $\bar{w}$ remains constant regardless of the a/b ratio, this is for all laminated composites structure and CNT graded configuration. However, the anti-symmetric square two-layer plates record the largest transverse displacement.

Figure 3 depicts the transverse displacement w/h of square simply supported FG-CNTRC plates versus the side to thickness ratio a/h for cross-ply symmetric [0°/90°/0°] laminated composites under nonlinear and combined temperature distribution for two (UD, FG-V) CNT graded configuration with the CNT volume fraction $V_{cnt}^{*} = 0.14$. In the part (a) of this figure, the nonlinear temperature T_3 is fixed to 100. The central deflection increase linear smoothly with increasing side to thickness ratio a/h until reaches the value $a/h = 50$ which can be considered as an inflection point. Subsequently, the central deflection begins to rise more strongly, and this intensity increases with the increase of the linear temperature. The same observation can be recorded for part (b) of the figure 3. However, the nonlinear temperature rise T_3 affects more central deflection than the linear temperature T_2. Also, we can be seen that the type of UD graded configuration gives values of central bending higher than FG-V CNT graded configuration, indeed that returns to the adequate distribution of the CNT fibers in the case of FG-V CNT graded configuration compared to CNT- UD ones.

Figure 4 shows the transverse displacement $\bar{w}$ of rectangular simply supported FG-CNTRC plates as function as aspect ratio a/b for different values of CNTs volume fraction and different structure lamination subject to linear temperature distribution ($T_3 = 0$). We can easily see that the increases of aspect ratio a/b lead to increasing of central deflection. This increasing is significant in the interval 0.5 to 2; from this latter the transverse displacement is almost constant. In addition the increasing of CNT fibers leads to a significant decrease in the transverse displacement $\bar{w}$, and this is due to the fact that the fibers are characterized by high elastic module, which increases the stiffness of the composite plate.

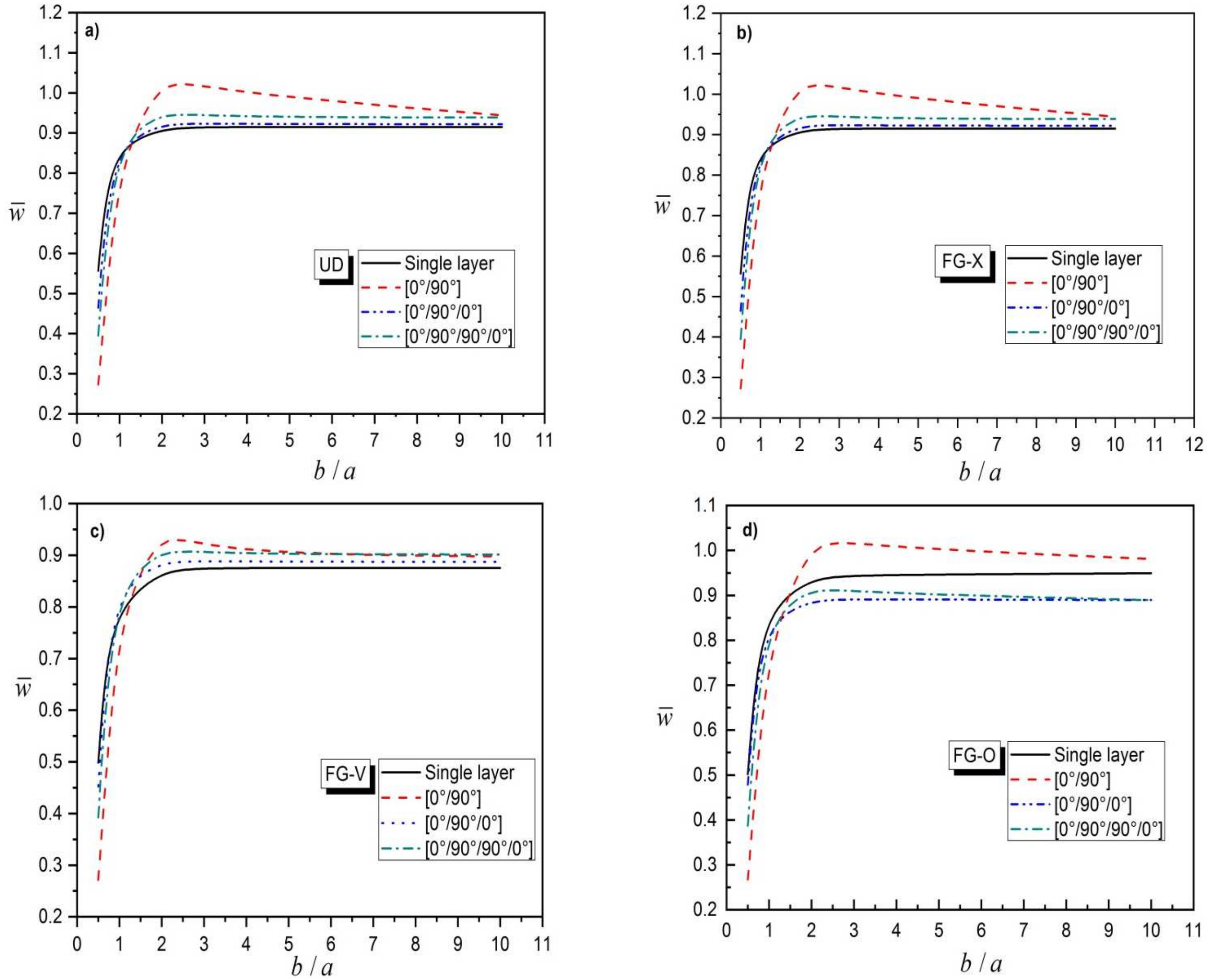

Fig. 2. Transverse displacement $\bar{w}$ of rectangular simply supported FG-CNTRC plates as function of aspect ratio a/b for different laminated composites structure subject to linear temperature $(T_2 = 100; T_3 = 0)$ distribution with ($V_{cnt}^{*} = 0.11$, a/h=10): a) UD, b) FG-X, c) FG-V, d) FG-O.

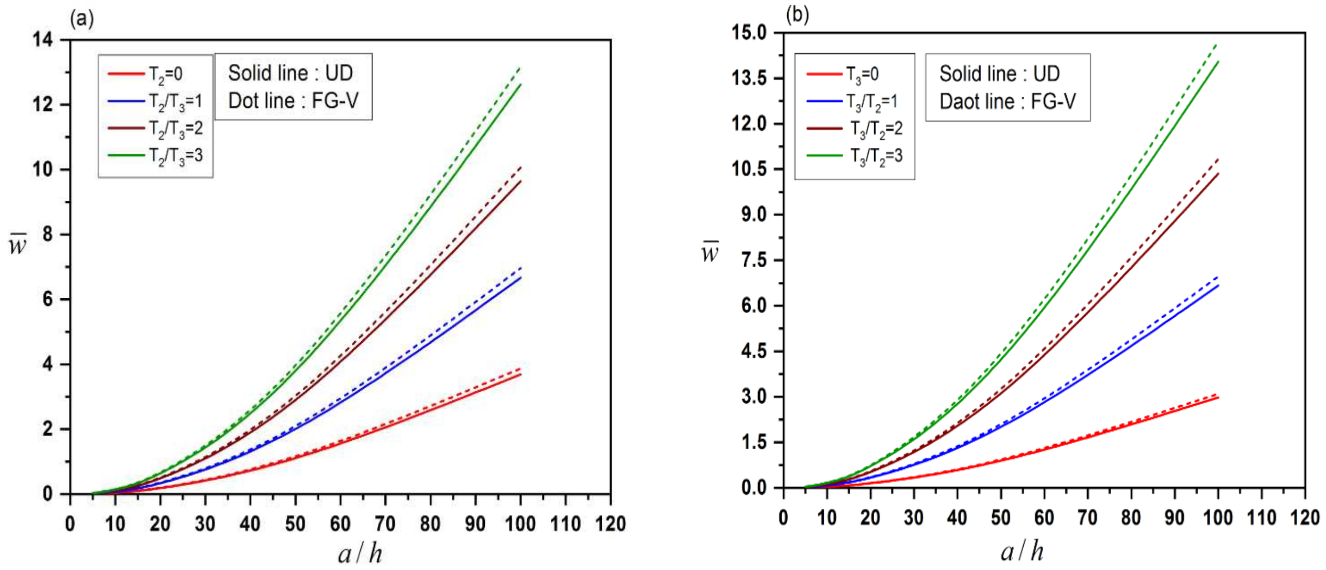

Fig. 3. Transverse displacement $\overline{w}$ of square simply supported FG-CNTRC plates versus the thickness ratio a/h for cross-ply symmetric [0°/90°/0°] laminated composites under, nonlinear and combined temperature distribution with $V_{cnt}^{*} = 0.14$: a) $T_3 = 100$, b) $T_2 = 100$

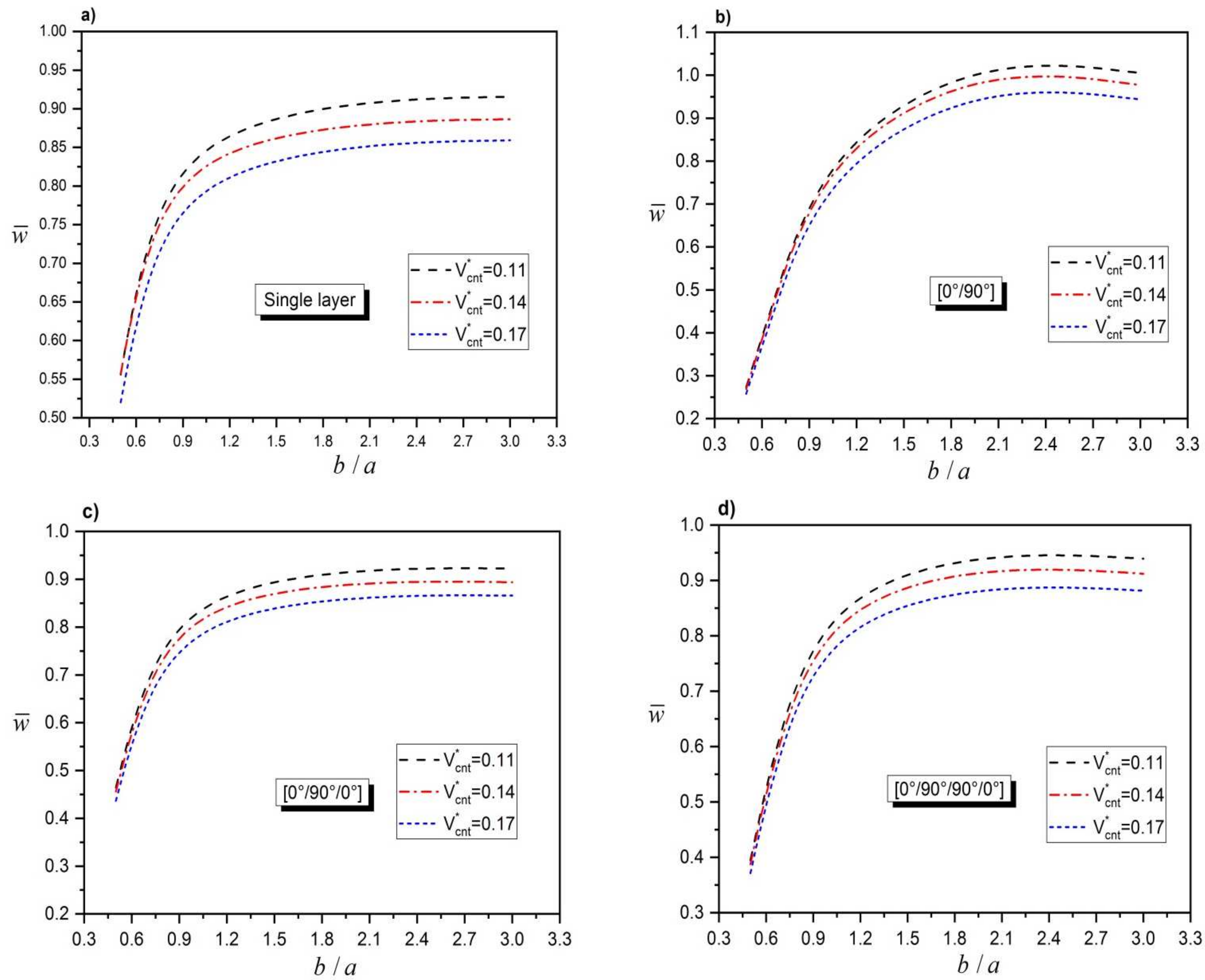

Fig. 4. Transverse displacement $\overline{w}$ of rectangular simply supported FG-CNTRC plates as function as aspect ratio a/b for different values of CNTs volume fraction and different laminated composites structure subject to linear temperature distribution ($T_3 = 0$).

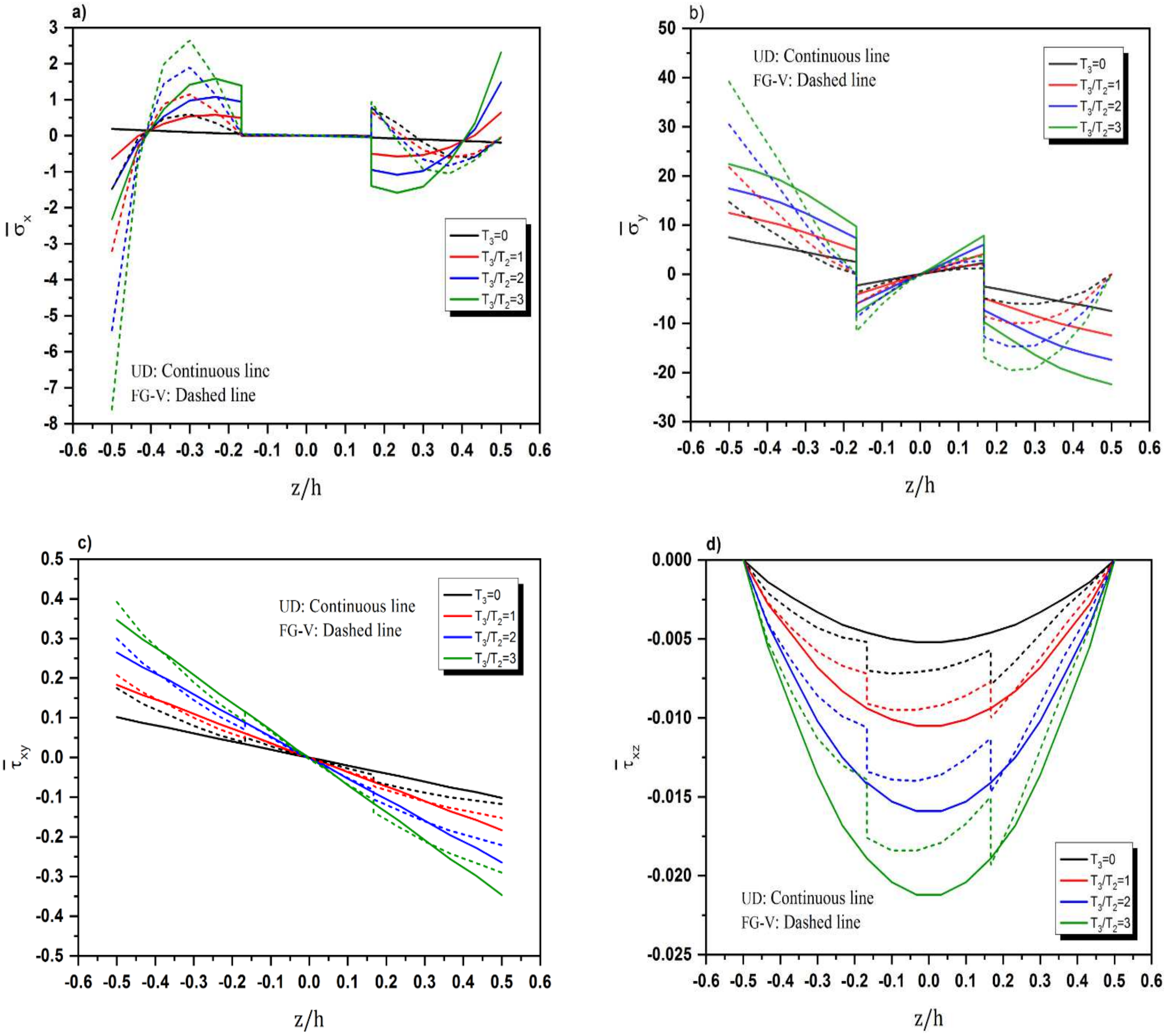

Fig. 5. Thermal stresses distribution across thickness of cross-ply [0°/90°/0°] simply supported square FG-CNTRC laminated plates subject to a nonlinear and combined temperature distribution ($T_2 = 100$) with $V^*_{cnt} = 0.14$, a/h=10 .

Figure 5 shows thermal stresses distribution across thickness of cross-ply [0°/90°/0°] simply supported square FG-CNTRC laminated plates subject to a nonlinear and combined temperature distribution ($T_2 = 0$) for two (UD and FG-V) CNT grade configuration with $V^*_{cnt} = 0.14$, a/h=10 . These results reveal that the variation of stresses is very sensitive to the variation of the nonlinear temperature distribution T_3 whether for thermal axial stresses $\bar{\sigma}_{xx}, \bar{\sigma}_{yy}$ or thermal shear stresses $\bar{\tau}_{xy}$, $\bar{\tau}_{xz}$. Also, it can be observed a high concentration of the thermal stresses at the laminate interfaces especially in the FG-CNT cases.

In Fig. 6 we plot the thermal stresses distribution across thickness of symmetric cross-ply [0°/90°/90°/0°] simply supported square FG-CNTRC laminated plates for different CNT distribution fibers types and subject to a linear temperature ($T_2 = 100$) with $V^*_{cnt} = 0.17$, a/h=10 It can be seen that CNTFG-V gives greater values for thermal stresses except for transverses thermal shear stresses $\bar{\tau}_{xz}$ that are high in the case of CNTFG-X, the maximum value of stresses $\bar{\tau}_{xz}$ occurs at a point on the mid-plane for all cases of CNT grading configurations fibers (UD, FG-X,O,V).

6. Conclusion

A new mathematical model based on the new higher shear deformation plate theory was developed to investigate the bending of carbon nanotube reinforced composites (CNTRC) cross-ply laminated plates under sinusoidal temperature loading. Linear, nonlinear, and combined variations of temperature through plate thickness direction were considered. The governing equations were derived from the principle of virtual displacement and solved analytically using Navier solution. A uniform distribution (UD) and three functionally graded distributions (FG) were inspected. The nano-scale effect of the CNT was taken into account by considering the efficiency parameters of the CNT. A comprehensive parametric study was carried out to show the influence of CNT volume fraction, laminated composites structure, side to thickness ratio, and aspect ratio on the thermal stresses and deflection of the CNTRC cross-ply laminated plates. Furthermore, it turned out through this study that:

- The increasing of CNT volume fraction leads to a significant decrease in the transverse displacement $\bar{w}$ values of CNTRC laminated plates.

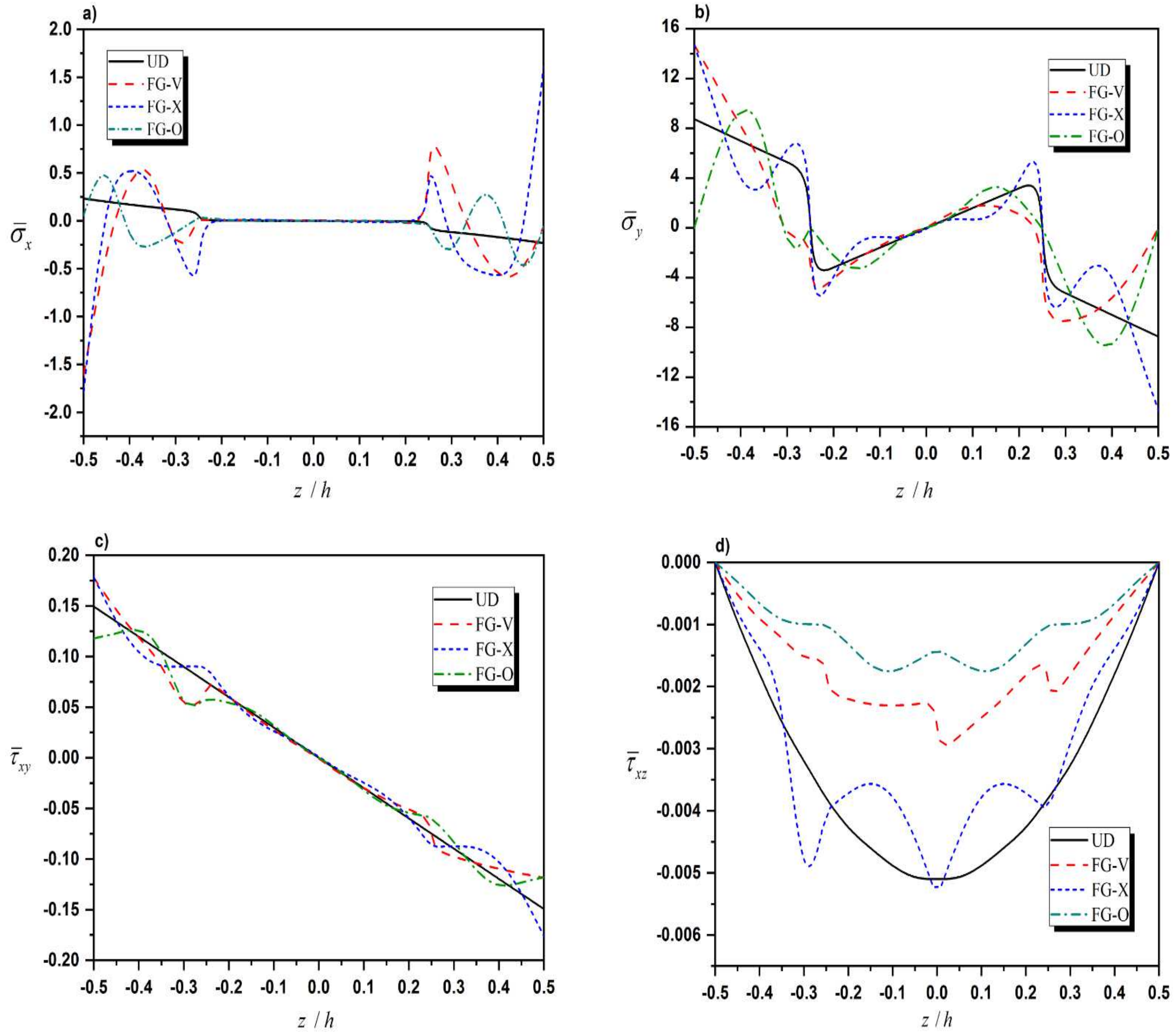

Fig. 6. Thermal stresses distribution across thickness of cross-ply [0°/90°/90°/0°] simply supported square FG-CNTRC laminated plates for different CNT distribution fibers types and subject to linear temperature ($T_2 = 100$) with $V^*_{cnt} = 0.17$, a/h=10 .

- The thermal stresses are very sensitive to the variation of the nonlinear temperature distribution. Therefore, the nonlinear term of temperature distribution should be taken into account for the bending of CNTRC laminated plates subjected to thermal loading.
- From a design point of view, it appears that the laminated composite structure [0°/90°] makes the CNTRC plates more susceptible to thermal transverse displacement compared to other laminations structure considering the same dimensions and material properties see Fig. 2.

Finally, it can be said that the proposed mathematical model based on new higher shear deformation plate theory that contains only four unknowns is of great importance to the designers who deal with carbon nanotube reinforced composites (CNTRC) cross-ply laminated plates subject to thermal loading in order to obtain good results for calculating the bending and thermal stresses required with reduced calculation cost time for their application.

Author Contributions

A. Bachiri planned the article, developed mathematical equations and results discussion; A.A. Daikh conducted the numerical programming and performed the validation phase of the mathematical model; A. Tounsi supervised the research. The manuscript was written through the contribution of all authors. All authors discussed the results, reviewed, and approved the final version of the manuscript.

Acknowledgments

The authors are grateful to Dr. Mohamed Mekerbi, Associated Professor at Setif University, Algeria, for providing some support and the fruitful conversations in order to realize this research.

Conflict of Interest

The authors declared no potential conflicts of interest concerning the research, authorship, and publication of this article.

Funding

The authors received no financial support for the research, authorship and publication of this article.

Data Availability Statements

The data sets generated and/or analyzed during the current study are available from the corresponding author on reasonable request.

Nomenclature

CNTRC	Carbon nanotube reinforced composite	γ_{ij}	Transverse deformation
V_{cnt}^{*}	Given volume fraction of CNT	σ_{ij}	Axial stress
V_{cnt}	Functionally graded volume fraction of CNT	τ_{ij}	Shear stress
W_{cnt}	CNTs mass fraction	A	Top surface plate
ρ	Mass density	N_{ij}	Total in-plane force resultants
E_{ij}	Elastic modulus	M_{ij}^{b}	Stress couples
$\bar{Q}_{ij}^{k}$	Transformed material constants	M_{ij}^{s}	Additional stress couples
θ	Oriented angles of fibers	Q_{ij}	Transverse shear stress resultants
G_{ij}	Shear modulus	$A_{ij}, B_{ij}, \ldots, H_{ij}$	Composite plate stiffness
ν_{ij}	Poisson's ratio	N_{ij}^{T}	Stress resultant due to thermal loading
η_{i}	CNT efficiency parameters	M_{i}^{bT}	Bending moment resultant due to thermal loading
V^{k}	Volume fraction of layer k	M_{i}^{sT}	Shear moment resultant due to thermal loading
α_{ij}	Thermal expansion coefficient	$T(x,y,z)$	Temperature field variation
u_0, v_0, w_0	Displacement components	U_{mn}, V_{mn}, W_{mn} and Ψ_{mn}	Unknown arbitrary parameters
ϕ	Rotation	$[L]$	Stiffness matrix
$f(z)$	Shape function	$\{\Lambda\}$	Unknown arbitrary parameters vector
ε_{ij}	Axial deformation	$\{F\}$	Thermal loading vector

References

[1] Sayyad, A.S., Shinde, B.M., and Ghugal, Y.M., Thermo-elastic bending analysis of laminated composite plates according to various shear deformation theories, *Open Engineering*, 5(1), 2015, 18–30.
[2] Shen, H.S., The effects of hygro-thermal conditions on the dynamic response of shear deformable laminated plates resting on elastic foundations, *Journal of Reinforced Plastics and Composites*, 23(10), 2004, 1095-1113.
[3] Bouazza, M., Kenouza, Y., Benseddiq, N., Zenkour, A.M., A two-variable simplified nth-higher-order theory for free vibration behavior of laminated plates, *Composite Structures*, 182, 2017, 533-541.
[4] Fidelus, J.D., Wiesel, E., Gojny, F.H., Schulte, K., Wagner, H.D., Thermo-mechanical properties of randomly oriented carbon/epoxy nanocomposites, *Composites Part A*, 36(11), 2005, 1555–61.
[5] Bonnet, P., Sireude, D., Garnier, B., Chauvet, O., Thermal properties and percolation in carbon nanotube–polymer composites, *Journal of Applied Physics*, 91(20), 2007, 201910.
[6] Han, Y., Elliott, J., Molecular dynamics simulations of the elastic properties of polymer/carbon nanotube composites, *Computational Materials Science*, 39(2), 2007, 315–323.
[7] Zhu, R., Pan, E., Roy, A.K., Molecular dynamics study of the stress–strain behavior of carbon-nanotube reinforced Epon 862 composites, *Materials Science and Engineering: A*, 447(1-2), 2007, 51–7.
[8] Wang Z.X., Shen H.S., Nonlinear vibration of nanotube-reinforced composite plates in thermal environments, *Computational Materials Science*, 50(8), 2011, 2319–2330
[9] Zarei, H., Fallah, M., Bisadi, H., Daneshmehr, A., Minak, G., Multiple impact response of temperature-dependent carbon nanotube -reinforced composite (CNTRC) plates with general boundary conditions, *Composites Part B*, 113, 2017, 206-217.
[10] Benguediab, S., Tounsi, A., Zidour, M., Abdelwahed, S., Chirality and scale effects on mechanical buckling properties of zigzag double-walled carbon nanotubes , *Composites Part B*, 57, 2014, 21-24.
[11] Salem. D., Synthèse de nanotubes de carbone mono-feuillets individuels et composites modèles polymers nanotubes de carbone. Application à l'effet photovoltaïque, *Ph.D thesis, University of Strasbourg*, 2012, (In French).
[12] Qian, D., Dickey, E.C., Andrews, R., Rantell, T., Load transfer and deformation mechanisms in carbon nanotubes-polystyrene composites, *Applied Physics Letters*, 76(20), 2000, 2868-2870.
[13] Zhu, P., Lei, Z.X., and Liew, K.M., Static and free vibration analyses of carbon nanotube-reinforced composite plates using finite element method with first order shear deformation plate theory, *Composite Structure*, 94(4), 2012, 1450-1460.
[14] Farazin, A., Aghadavoudi, F., Motififard, M., Saber-Samandari, S., Khandan, A., Nanostructure, Molecular Dynamics Simulation and Mechanical Performance of PCL Membranes Reinforced with Antibacterial Nanoparticles, *Journal of Applied and Computational Mechanics*, 7(4), 2021, 1907–1915.
[15] Popov, V.N., Doren, V.E.V., and Balkanski, M., Elastic properties of crystals of single-walled carbon nanotubes, *Solid State Communication*, 114(7), 2000, 395-399.
[16] Draoui, A., Zidour, M., Tounsi, A., Adim, B., Static and dynamic behavior of nanotubes-reinforced sandwich plates using (FSDT), *Journal of Nano Research*, 57, 2019, 117–135.
[17] Alibeigloo, A., Liew, K.M., Thermo-elastic analysis of functionally graded carbon nanotube-reinforced composite plate using theory of elasticity, *Composite Structure*, 106, 2013, 873-881.
[18] Bakhti, A., Kaci, A., Bousahla, A.A., Houari, M.S.A., Tounsi, A., Adda Bedia, E.A., Large deformation analysis for functionally graded carbon

nanotube-reinforced composite plates using an efficient and simple refined theory, *Steel and Composite Structures*, 14(4), 2013, 335-347.
[19] Zerrouki, R., Karas, A., Zidour, M., Bousahla, A.A., Tounsi, A., Bourada, F., et al., Effect of nonlinear FG-CNT distribution on mechanical properties of functionally graded nano-composite beam, *Structural Engineering and Mechanics*, 78(2), 2021, 117-124.
[20] Sobhy, M., Levy solution for bending response of FG carbon nanotube reinforced plates under uniform, linear, sinusoidal and exponential distributed loadings, *Engineering Structures*, 182, 2019, 198–212.
[21] Zeverdejani, M. K., Beni, Y.T., Effect of laminate configuration on the free vibration/buckling of FG Graphene/PMMA composites, *Advances in Nano Research*, 8(2), 2020, 103-114.
[22] Zeverdejani, M.K., Beni, Y.T., Kiani, Y., Multi-scale buckling and post-buckling analysis of functionally graded laminated composite plates reinforced by defective graphene sheets, *International Journal of Structural Stability and Dynamics*, 20(01), 2020, 2050001.
[23] Kiani, Y., Torsional vibration of functionally graded carbon nanotube reinforced conical shells, *Science and Engineering of Composite Materials*, 25(1), 2018, 41–52
[24] Long, V.T., Tung, H.V., Thermal postbuckling behavior of CNT-reinforced composite sandwich plate models resting on elastic foundations with tangentially restrained edges and temperature dependent properties, *Journal of Thermoplastic Composite Materials*, 33(10), 2020, 1396-1428.
[25] Han, J.W., Kim, J.S., Cho, M., New enhanced first-order shear deformation theory for thermo-mechanical analysis of laminated and sandwich plates, *Composites Part B*, 116, 2016,422-450.
[26] Daikh, A.A., Bachiri, A., Houari, M.S.A., Tounsi, A., Merzouki, T., On static bending of multilayered carbon nanotube Reinforced composite plates, *Computers and Concrete*, 26(2), 2020, 137-150.
[27] Fazzolari, F.A., Banerjee, J.R., Boscolo, M., Buckling of composite plate assemblies using higher order shear deformation theory-An exact method of solution, *Thin-Walled Structure*, 71, 2013, 18-34.
[28] Khdeir, A.A., Reddy, J.N., Thermal stresses and deflections of cross-ply laminated plates using refined plate theories, *Journal of Thermal Stresses*, 14(4), 1991,419-438.
[29] Zenkour, A.M., Analytical solution for bending of cross-ply laminated plates under thermo-mechanical loading, *Composite Structures*, 65(3-4), 2004, 367–379.
[30] Shen, H.S., Nonlinear bending of functionally graded carbon nanotube-reinforced composite plates in thermal environments, *Composite Structures*, 91(1), 2009, 9-19.
[31] Bakhadda, B., Bouiadjra, B.M., Bourada, F., Bousahla, A.A., Tounsi, A., Mahmoud, S.R., Dynamic and bending analysis of carbon nanotube-reinforced composite plates with elastic foundation, *Wind and Structures*, 27(5), 2018, 311–324.
[32] Naik, N.S., Sayyad, A.S., An accurate computational model for thermal analysis of laminated composite and sandwich plates, *Journal of Thermal Stresses*, 42(5), 2019, 559-579.
[33] Kaci, A., Tounsi, A., Bakhti, K., Adda Bedia, E.A., Nonlinear cylindrical bending of functionally graded carbon nanotube-reinforced composite plates, *Steel and Composite Structures*, 12(6), 2012, 491-504.
[34] Kamarian, S., Bodaghi, M., Isfahani, R.B., Song, J.I., Thermal buckling analysis of sandwich plates with soft core and CNT-Reinforced composite face sheets, *Journal of Sandwich Structures & Materials*, 23(8), 2021, 3606-3644.
[35] Daikh, A.A., Megueni, A., Thermal buckling analysis of functionally graded sandwich plates, *Journal of Thermal Stresses*, 41(2), 2018, 139–159.
[36] Daikh, A.A., Houari, M.S.A., Tounsi, A., Buckling analysis of porous FGM sandwich nanoplates due to heat conduction via nonlocal strain gradient theory, *Engineering Research Express*, 1(1), 2019, 015022
[37] Daikh, A.A., Guerroudj, M., ElAdjrami, M., Megueni, A., Thermal Buckling of Functionally Graded Sandwich Beams, *Advanced Materials Research*, 1156, 2019, 43–59.
[38] Daikh, A.A., Zenkour, A.M., Effect of porosity on the bending analysis of various functionally graded sandwich plates, *Materials Research Express*, 6(6), 2019, 065703.
[39] Houari, M.S.A, Benyoucef, S., Mechab, T., Tounsi, A., Bedia, E.A.A., Two-Variable Refined Plate Theory for Thermoelastic Bending Analysis of Functionally Graded Sandwich Plates, *Journal of Thermal Stresses*, 34(4), 2011, 315-334.
[40] Zidi, M., Tounsi, A., Houari, M.S.A., Adda Bedia, E.A., Bég, A., Bending analysis of FGM plates under hygro-thermo-mechanical loading using a four variable refined plate theory, *Aerospace Science and Technology*, 34, 2014, 24–34.
[41] Pashmforoush, F., Finite element analysis of low velocity impact on carbon fibers/carbon nanotubes reinforced polymer composites, *Journal of Applied and Computational Mechanics*, 6(3), 2020, 383-393.
[42] Mehar, K., Panda, S.K., Theoretical deflection analysis of multi-walled carbon nanotube reinforced sandwich panel and experimental verification, *Composites Part B*, 167, 2019, 317-328.
[43] Adhikari, B., Singh, B.N., Thermo-elastic analysis of laminated functionally graded CNT plates, *AIAA SciTech Forum*, 7(11), 2019, 1-23.
[44] Akbas, S.D., Kocatürk, T., Post-buckling analysis of functionally graded three-dimensional beams under the influence of temperature, *Journal of Thermal Stresses*, 36(12), 2013, 1233-1254.
[45] Akbas, S.D., Free vibration of axially functionally graded beams in thermal environment, *International Journal of Engineering and Applied Sciences*, 6(3), 2014, 37-51.
[46] Reddy, J.N., Hsu, Y.S., Effects of shear deformation and anisotropy on the thermal bending of layered composite plates, *Journal of Thermal Stresses*, 3(4), 1980, 475-493.
[47] Ansari, M.I., Kumar, A., Bending analysis of functionally graded CNT reinforced doubly curved singly ruled truncated rhombic cone, *Mechanics Based Design of Structures and Machines*, 47(1), 2019, 67-86.
[48] Ansari, M.I., Kumar, A., Flexural analysis of functionally graded CNT-reinforced doubly curved singly ruled composite truncated cone, *Journal of Aerospace Engineering*, 32(2), 2019, 04018154.
[49] Ansari, M.I., Kumar, A., Fic, S., Barnat-Hunek, D., Flexural and free vibration analysis of CNT-reinforced functionally graded plate, *Materials*, 11(12), 2018, 2387.
[50] Ansari, M.I., Kumar, A., Barnat-Hunek, D., Suchorab, Z., Andrzejuk, W., Majerek, D., Static and dynamic response of FG-CNT-reinforced rhombic laminates, *Applied Sciences*, 8(5), 2018, 834.
[51] Chaubey, A.K., Kumar, A., Chakrabarti, A., Vibration of laminated composite shells with cutouts and concentrated mass, *AIAA Journal*, 56(4), 2018, 1662-1678.
[52] Chaubey, A.K., Kumar, A., Mishra, S.S., Dynamic analysis of laminated composite rhombic elliptic paraboloid due to mass variation, *Journal of Aerospace Engineering*, 31(5), 2018, 04018059.
[53] Anish, K.A., Chakrabarti, A., Influence of openings and additional mass on vibration of laminated sandwich rhombic plates using IHSDT, *Journal of Thermoplastic Composite Materials*, 33(1), 2020, 3-34.
[54] Akbas, S.D., Large deflection analysis of a fiber reinforced composite beam, *Steel and Composite Structures*, 27(5), 2018, 567-576.
[55] Akbas, S.D., Nonlinear static analysis of laminated composite beams under hygro-thermal effect, *Structural Engineering and Mechanics*, 72(4), 2019, 433-441.
[56] Akbas, S.D., Dynamic analysis of a laminated composite beam under harmonic load, *Coupled Systems Mechanics*, 9(6), 2020, 563-573.
[57] Akbas, S.D., Forced vibration analysis of a fiber reinforced composite beam, *Advances in Materials Research*, 10(1), 2021, 57-66.
[58] Nguyen, P.D., Papazafeiropoulos, G., Vu, Q.V., Duc, N.D., Buckling response of laminated FG-CNT reinforced composite plates: Analytical and finite element approach, *Aerospace Science and Technology*, 2022, 107368.
[59] Reddy, J.N., *Mechanics of Laminated Composite Plates and Shells: Theory and Analysis*, CRC Pres, New York, 2004.
[60] Fazzolari, F.A., Thermo-elastic vibration and stability of temperature-dependent carbon nanotube-reinforced composite plates, *Composite Structures*, 196, 2018, 199-214.
[61] Bourada, F., Amara, K., Tounsi, A., Buckling analysis of isotropic and orthotropic plates using a novel four variable refined plate theory, *Steel and Composite Structures*, 21(6), 2016, 1287-1306.
[62] Mahmoudi, A., Benyoucef, S., Tounsi, A., Benachour, A., Bedia, E.A.A., On the effect of the micromechanical models on the free vibration of rectangular FGM plate resting on elastic foundation, *Earthquakes and Structures*, 14(2), 2018, 117-128.
[63] Bachiri, A., Bourada, M., Mahmoudi, A., Benyoucef, S., Tounsi, A., Thermodynamic effect on the bending response of elastic foundation FG plate by using a novel four variable refined plate theory, *Journal of Thermal Stresses*, 41(8), 2018, 1042–1062.

ORCID iD

Attia Bachiri https://orcid.org/0000-0002-2402-0490
Ahmed Amine Daikh https://orcid.org/0000-0002-4666-2750
Abdelouahed Tounsi https://orcid.org/0000-0002-5601-3228

How to cite this article: Bachiri A., Daikh A.A., Tounsi A., On the thermo-elastic response of FG-CNTRC cross-ply laminated plates under temperature loading using a new HSDT, *J. Appl. Comput. Mech.*, 8(4), 2022, 1370–1386. https://doi.org/10.22055/jacm.2022.40148.3529